Investigation of sphenoid spine morphometry for skull base surgery and relation to foramen spinosum localization

Eda Duygu Ipek, Berrin Ozustun, Ilgaz Akdogan

Aydin Adnan Menderes University, Faculty of Medicine, Department of Anatomy, Aydin, Turkey

SUMMARY

Our study aimed to investigate the sphenoid spine morphological characterization, as well as the distances to important surgical points and its relation to foramen spinosum localization. On a total of 65 skulls, the distances of the sphenoid spine to various surgically important anatomical landmarks were measured from both the right and left sides. The length of the sphenoid spine was measured and classified morphologically. Localization of the foramen spinosum relation to the sphenoid spine was evaluated. The sphenoid spine length was statistically different which was found to be 6.71±1.97 and 6.14±1.93 on the right and left sides, respectively (p=0.027). The most commonly encountered shape of the sphenoid spine on both sides was quadrangular, followed by spine shape. The foramen spinosum was most frequently located anteromedially and least frequently located anterolaterally in relation to the sphenoid spine. In our study, it was determined that the localization of the foramen spinosum is associated with the shape of the sphenoid spine, on both the right (p=0.012) and left (p=0.016) sides. Our study provides morphometric data on the sphenoid spine and reports the association between the localization of the foramen spinosum and the type of sphenoid spine.

Key words: Sphenoid spine – Foramen spinosum – Infratemporal fossa – Endoscopic approach – Skull base

INTRODUCTION

The sphenoid spine, described as spina ossis sphenoidalis in anatomical terminology, is a pointed protrusion extending downward from the junction of the squamosal and posterior borders of the greater wings of the sphenoid bone. Three ligaments, ligamentum sphenomandibulare, mallei anterius and pterygospinosus, two muscles, musculus tensor veli palatini and tensor tympani, are attached to the sphenoid spine. Furthermore, it is adjacent to the cartilaginous part of the external auditory canal and chorda tympani medially, and to the auriculotemporal nerve laterally (Infant Reshawn and Yuvaraj Babu, 2020).

Technological advancements have significantly expanded the range of areas accessible through endoscopic approaches in skull base surgeries, but the complications attributed to these

Corresponding author:
Asst. Prof. Eda Duygu Ipek. Aydin Adnan Menderes University, Faculty of Medicine, Department of Anatomy, Efeler 09010, Aydin, Turkey. Phone: +90 545 684 86 73; Fax: +90 256 212 31 69. E-mail: eda.cakir@adu.edu.tr

Submitted: March 12, 2024. **Accepted:** March 31, 2024

https://doi.org/10.52083/KGHN8857

approaches have also increased proportionally (Fang et al., 2020). The internal carotid artery (ICA) is the most feared structure by endoscopic surgeons for its complications in skull base surgeries. In particular, there is a lack of anatomical landmarks that allows the safe exposure of the cervical portion of the ICA, which is surrounded by soft tissues throughout the parapharyngeal area in infratemporal fossa, and access to this segment of the ICA is less defined (Liu et al., 2019; Fang et al., 2020). In endoscopic transpterygoid approach, the pterygoid plate, mandibular nerve, Eustachian tube, and styloid process have been reported as reliable landmarks for reaching the parapharyngeal ICA (Falcon et al., 2011). Liu et al. (2014) reported that the sphenoid spine and foramen spinosum are anatomical landmarks for the cartilaginous and bony junction of the Eustachian tube, and parapharyngeal ICA was located immediately posteroinferior to the sphenoid spine. Liu et al. (2019) also found that the sphenoid spine, tympanic crest and vaginal process of tympanic bone were the closest anatomical landmarks to the parapharyngeal ICA in the endoscopic transmasticator approach. Li et al. (2022) reported that in transoral nasopharyngectomy, it is mandatory to define the parapharyngeal ICA before transection of the Eustachian tube, and the best landmarks defining it are the sphenoid spine, the petrotympanic fissure and the pterigoid hamulus.

The foramen spinosum, through which the middle meningeal vessels and the meningeal branch of the mandibular nerve pass to middle cranial fossa, is located in the greater wing of the sphenoid bone. It is named 'spinosum' due to its close proximity to the sphenoid spine, and it is described in classical anatomy texts to be located on the anteromedial side of sphenoid spine (Worku and Clarke, 2021; Sugano et al., 2022; Sink et al., 2023). Although it has been evaluated in very few studies in the literature, it is observed that the localization of foramen spinosum varies relation to the sphenoid spine (Sophia and Kalpana, 2015; Worku and Clarke, 2021; Sink et al., 2023). The localization of the foramen spinosum is important in various procedures, such as endovascular embolization of dural arteriovenous fistulas and meningiomas through the middle meningeal artery (Sink et al., 2023), in bypass operations where middle meningeal artery is used as a graft (Sophia and Kalpana, 2015). Also, it has been reported that anatomical variations of the foramen spinosum may be associated with abnormal development of the middle meningeal artery (Sugano et al., 2022). Therefore, a more detailed understanding of the localization of the foramen spinosum is necessary in the preoperative assessment of possible changes in the trajectory of neurovascular structures. The sphenoid spine is used as a landmark during infratemporal surgical approaches due to its close proximity to the foramen spinosum, parapharyngeal ICA, Eustachian tube and chorda tympani (Worku and Clarke, 2021). Despite its clinical importance, there is a lack of data in the literature regarding the anatomical variations of the sphenoid spine, and studies investigating its relationship with adjacent structures are insufficient. In the present study, considering the importance of the topography of the sphenoid spine and foramen spinosum in skull base surgeries, to the aim was to examine in more detail the relation between the foramen spinosum to the sphenoid spine, as well as the morphometric analysis of sphenoid spine with related structures.

MATERIALS AND METHODS

In this study, 65 adult skulls of unknown gender, obtained from the bone archive of Aydin Adnan Menderes University, Faculty of Medicine, Department of Anatomy, were used. Damaged skulls that did not allow examination of the targeted structures were not included in the study. The distance of the sphenoid spine to the tip of mastoid process (SMP), to the tip of tuberculum articulare (STA), to the anterior border of the external orifice of the carotid canal (SCC), to the point where the sutura sphenosquamosa intersects the crista infratemporalis (SO), to the most lateral (SPFl) and medial (SPFm) endpoints of the petrotympanic fissure, to the sphenoidal tubercle (STS), and the length of the sphenoid spine (SL) were measured on the right and left sides, using a digital Vernier caliper (eSynic, Hong Kong, China) with a precision of 0.01 mm.

The morphological characterization of the sphenoid spine was classified into five types: spine, quadrangular, pyramidal, plate and cup-shaped, as shown in Fig. 1.

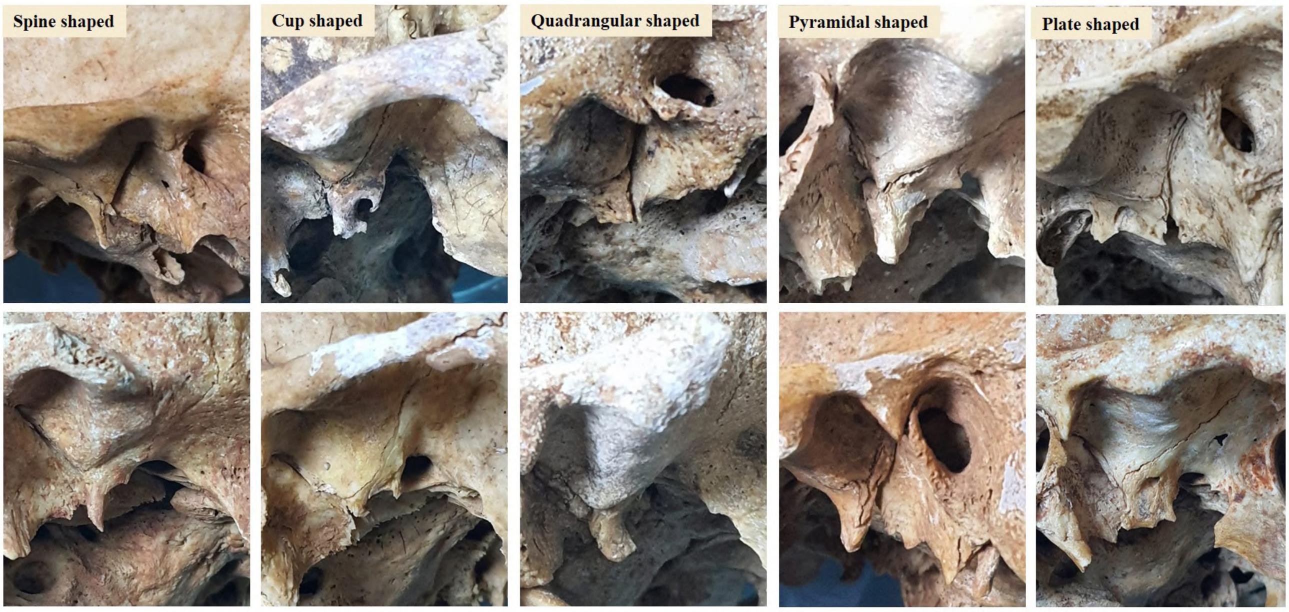

Fig. 1.- Examples of sphenoid spine morphological types.

The localization of the foramen spinosum relation to the sphenoid spine was examined from the basis cranii externa. A sagittal line was passed through the center of the foramen spinosum as shown in Fig. 2. The location of the foramen spinosum was classified as medial (M), lateral (L), anterior (A), anteromedial (AM), anterolateral (AL) and anterior-on-the-line (AO), medial-on-the-line (MO) and lateral-on-the-line (LO). In M and L placement, the line passed through the medial and lateral sides of the sphenoid spine while intersected with the sphenoid spine in A placement. In the AM and AL placement, the foramen spinosum was in front of the sphenoid spine and the line was on the medial and lateral sides of the sphenoid spine, respectively. Skulls with a line transition similar to the M, L and A placement of the foramen spinosum, but where the middle meningeal artery groove was observed on the sphenoid spine root, were classified as MO, LO and AO, respectively.

SPSS (Version 22.0, SPSS Inc., Chicago, IL, USA) program was used for statistical analysis of the data. The distribution pattern of the data was evaluated with the Kolmogorov Smirnov test, and paired-t test was applied to compare the right and left morphometric parameters. Chi-square test

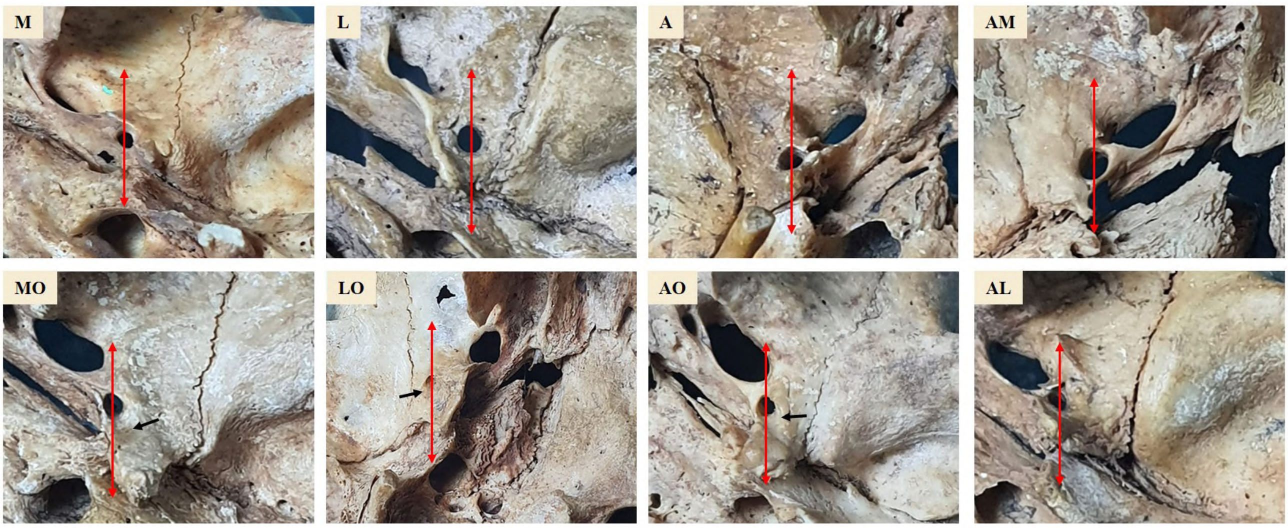

Fig. 2.- The foramen spinosum localization in relation to the sphenoid spine: medial (M), lateral (L), anterior (A), anteromedial (AM), anterolateral (AL) and anterior-on the line (AO), medial-on the line (MO) and lateral-on the line (LO). The black arrows show the middle meningeal artery groove observed at the root of the sphenoid spine.

Table 1. Mean, minimum and maximum values of morphometric parameters. See material and methods section for abbreviations.

	Right side mean±sd (min–max) n=65	**Left side mean±sd (min–max) n=65**	**p value (Sig. 2-tailed)**
STA	29.08±2.67 (22.7-35.6)	28.57±2.36 (22.1-34.3)	0.71
SMP	32.97±2.79 (26.6-44,1)	33.67±2.93 (25.8-41.4)	0.63
SPFl	23.98±3.03 (17.5-30.4)	23.79±2.68 (18-29.6)	0.602
SPFm	4.05±1.27 (2.2-5.8)	4.21±1.27 (2.1-6.3)	0.512
SO	29.98±4.17 (21.3-40.4)	29.76±4.01 (20.7-39.9)	0.635
SCC	6.53±1.86 (2.2-11.1)	6.74±2.28 (2.4-12.4)	0.426
STS	33.13±3.57 (20.5-41.4)	33.37±4.94 (25.3-42.7)	0.729
SL	6.71±1.97 (2.3-10.7)	6.14±1.93 (2-10.4)	0.027

sd: standart deviation, The p values represent the diference between left and right sides

was used to evaluate the localization of the foramen spinosum according to sphenoid spine morphological types.

RESULTS

The descriptive statistics of the morphometric measurements we conducted are indicated in Table 1. In comparing the morphometric measurements between the right and left sides, it was found that only the length of the sphenoid spine was statistically higher on the right side (p=0.027).

The most commonly encountered morphological type of the sphenoid spine on both the right and left sides was quadrangular, 35.35% of the total, followed by a spine shape. On the left side, the least encountered morphological type of the sphenoid spine was plate-shaped (10.8%), while on the right side, it was cup-shaped (12.3%). We found that the tip of the sphenoid spine was bifurcated unilaterally in a total of 3 skulls (4.61%), one with pyramidal and two with quadrangular shape. Additionally, pterygospinous bar and pterygospinous foramen, formed by the ossification of the pterygopinous ligament, were detected unilaterally on two sides (1.53%). The mentioned variations are shown in Fig. 3. Morphometric measurement mean values and frequency of sphenoid spine types are given in Table 2.

Table 2. Morphometric parameters in sphenoid spine morphological types. See material and methods section for abbreviations.

	Spine		**Quadrangular**		**Pyramidal**		**Cup**		**Plate**	
	Right side n=15. 23.1%	Left side n=12. 18.5%	Right side n=22. 33.8%	Left side n=24. 36.9%	Right side n=10. 15.4%	Left side n=11. 16.9%	Right side n=11. 16.9%	Left side n=8. 12.3%	Right side n=7. 10.8%	Left side n=10. 15.4%
STA	27.91±2.16	27.84±2.08	29.81±2.84	28.9±2.58	29.02±25.5	29.2±2.01	29.4±2.05	28.1±1.92	28.6±3.84	28.1±2.81
SMP	32.6±2.44	32.3±3.41	33.3±3.66	33.8±2.55	32.06±1.6	33.8±2.64	33.38±1.87	35.1±3.85	33.2±3.21	33.4±2.5
SPFl	23.7±3.25	23.09±3.1	24.1±3.23	23.9±2.89	24.3±3.15	24.1±2.68	24.3±2.93	23.4±1.4	22.8±2.31	24.05±26
SPFm	4.97±1.12	4.12±0.8	3.96±0.75	4.01±1.04	4.62±1.2	4.34±0.92	3.92±0.76	4.3±1.11	3.2±0.76	3.5±0.88
SO	29.5±5.59	27.8±3.52	29.9±3.18	30.24±4.2	32.07±4.09	30.13±3.5	29.3±3.04	28.3±3.26	29.1±5.23	31.6±4.31
SCC	6.6±2.17	6.51±2.23	6.57±2.15	6.55±2.47	5.6±1.27	7.81±1.57	7.08±1.66	7.5±2.9	6.68±1.01	5.69±1.68
STS	32.4±3.51	32.36±3.9	33.2±3.36	33.5±2.63	34.8±2.31	35.38±2.7	32.9±3.14	33.31±4.11	32.1±6.02	31.89±10
SL	6.8±2.45	6.37±1.63	6.7±2.05	5.66±1.85	7.18±0.94	5.09±1.13	6.67±1.65	4.87±195	5.98±2.39	5.4±2.01

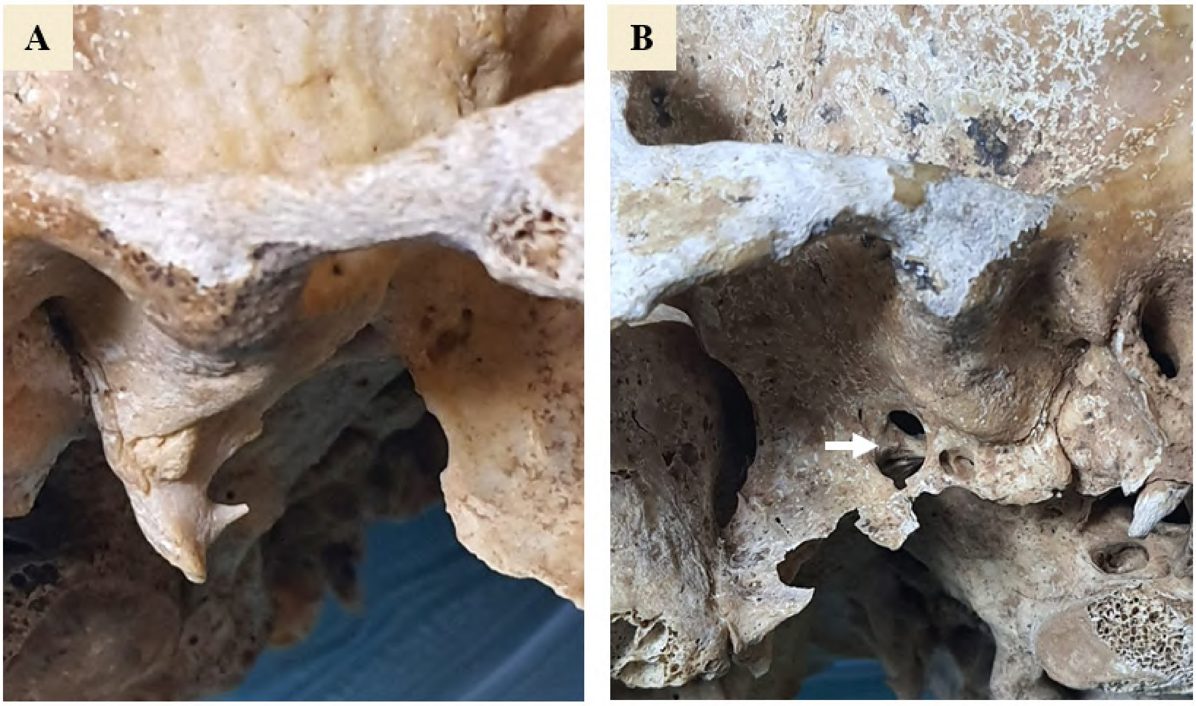

Fig. 3.- A: Bifurcated sphenoid spine. **B**: White arrow indicates pterygospinosus foramen (Civinini's foramen).

As shown in Table 3, it was determined that the foramen spinosum is frequently located in the anteromedial aspect of the sphenoid spine on both sides. It can be said that the foramen spinosum is frequently located anteromedially in skulls with spine, quadrangular, and pyramidal shapes of the sphenoid spine, while in plate shape, lateralization of the foramen spinosum is more commonly observed. According to the Chi-square test result, the localization of the foramen spinosum was associated with the morphological type of the sphenoid spine on both sides.

DISCUSSION

The safe exposure of the parapharyngeal segment of the ICA is necessary for many surgical procedures that will be performed through the infratemporal fossa. In addition to the sphenoid spine being an important anatomical landmark for identifying the internal carotid artery, its re-

Table 3. Foramen spinosum localisation according to sphenoid spine morphology: medial (M), lateral (L), anterior (A), anteromedial (AM), anterolateral (AL) and anterior-on the line (AO), medial-on the line (MO) and lateral-on the line (LO).

	A		M		L		MO		AM		AO		AL		LO		p
	Right %4.6	Left %4.6	Right %9.2	Left %9.2	Right %6.2	Left %6.2	Right %4.6	Left %1.5	Right %33.8	Left %38.5	Right %33.8	Left %26.2	Right %7.7	Left %10.8	Right -	Left %3.1	
Spine	1	0	1	1	0	0	2	1	5	6	6	3	0	0	0	1	**0.012a** **0.016b**
Quadrangular	0	3	1	1	0	2	1	0	10	9	9	8	1	0	0	1	
Pyramidal	1	0	1	1	0	0	0	0	5	6	2	4	1	0	0	0	
Cup	1	0	3	2	2	0	0	0	2	3	3	1	0	2	0	0	
Plate	0	0	0	1	2	2	0	0	0	1	2	1	3	5	0	0	

The Pearson Chi square p values represent the location of the foramen spinosum is related to the type of sphenoid spine on the right[a] and left[b] sides lationship with the position of the foramen spinosum is also clinically important. However, its anatomical variations and relationships with other structures in the infratemporal fossa have not been precisely elucidated.

In this study, we did not find statistical difference between the right and left sides in SMP and STA values similar to Infant Reshawn and Yuvaraj Babu (2020). They reported SMP values in 30 skulls as 30.56±1.10 mm and 30.66±1.12 mm, STA values as 22.07±2.12 mm and 22.13±2.12 mm, on the right and left sides, respectively. While the SMP values in our study are close to their findings, our STA values are higher. Liu and Yi (2020) defined the intersection point of the sphenosquamous suture with the infratemporal crest as ''point O', and reported that point O can be used as a reliable landmark in lateral skull base surgeries when other landmark points cannot be identified. Our distance values between the sphenoid spine and O point were not statistically different between the right and left sides. However, they were found to be distributed in a wide range, 21.3 mm-40.4 mm and 20.7 mm-39.9 mm, respectively. Another surgical reference point used in infratemporal fossa surgeries is a bony prominence located at the anterior end of the infratemporal crest, referred to as the sphenoidal tubercle in the literature. It is confused with the sphenoid spine in some studies (Stajcic et al., 2010; Rusu et al., 2019). Our mean STS values on the right and left sides were found to be quite close to each other. The lateral pterygoid muscle, the only muscle responsible for opening the jaw, attaches to the sphenoidal tubercle, and the sphenomandibular ligament, extending between the sphenoid spine and mandibular lingula, is tense when the jaw is open (Simonds et al., 2017). Therefore, the anatomy of the sphenoid spine and the sphenoidal tubercle may be related. Furthermore, it is reported that there is a close relationship between the temporomandibular joint and the middle ear, explained by the presence of the discomalleolar ligament, anterior mallear ligament and the sphenomandibulare ligament. It is considered that the presence of otological symptoms in patients with temporomandibular joint disorders may be associated with the petrotympanic fissure morphology and ossification. (Almaşan et al., 2022). We did not find difference for SPFm and SPFl between the right and left sides. As seen in Table 2, the SPFm distance was the lowest in plate-shaped sphenoid spines. Considering the frequent lateral placement of the foramen spinosum in these shapes, it can be said that, as mentioned by Sugano et al. (2022), the foramen spinosum is very close to the petrotympanic fissure in these skulls. Liu et al. (2019) reported that the distance from the sphenoid spine to the external orifice of the carotid canal, from 2.5 to 6.1 mm, was highly variable. Although our data are variably similar to their findings, ranged from 2.2 to 11.1 and 2.4 to 12.4 on the right and left sides, respectively, they reveal a significantly higher maximum value. Our SCC findings are closer to the values reported by Sink et al. (2023) as 8.02±1.35 mm (5.13 mm-13.60 mm) and 8.22±1.47 mm (5.04 mm-14.97 mm) on the right and left sides, respectively. Li et al. (2019) reported that the sphenoid spine length was also variable. We found that only the sphenoid spine length was statistically different between the right and left sides and our mean values are close to their finding of 5.98 mm. They reported that the tip of the sphenoid spine bifurcated in 10% of the specimens, which is higher than the rate of 3.07% we identified. However, they used only 10 skulls. Iwanaga et al. (2020), detected bony pterygospinosus bar on two sides (%6.66) in 15 cadaveric head specimens which was higher than our study (Fig. 3).

In the literature, only Infant Reshawn and Yuvaraj Babu (2020) categorized sphenoid spine morphology as sharp, rounded, blunt, and pointed in 30 skulls. However, they did not provide detailed information or examples related to this morphological classification in their reports. We classified sphenoid spine types into 5 categories, as seen in Fig. 1. Infant Reshawn and Yuvaraj Babu (2020) most commonly identified a rounded shape. Interestingly, we found that the sphenoid spine, which we know as a spiny protrusion, was often quadrangular shape not spiny. A significant association were found between the morphological shape of the sphenoid spine and the location of the foramen spinosum on both sides. Worku and Clarke (2021) and Sophia et al. (2015) classified the position of the foramen spinosum in relation to the sphenoid spine as normal (anteromedial), lateral, and medial placements. Worku and Clarke (2021) found that the foramen spinosum anteromedially located in 61 of a total of 64 skulls. Sophia et al. (2015) reported that the rate of anteromedial location of the foramen spinosum as 25% in 40 skulls on 80 sides. The total anteromedial placement percentage of our study is 36.15%, lower than Worku and Clarke (2021) and higher than Sophia et al. (2015). Worku and Clarke (2021) reported lateral and medial placement on 4 and 2 sides, respectively. Sophia et al. (2015) reported the highest lateral placement on 21 sides, medial placement on three sides. Sugano et al. (2022) detected laterally located foramen spinosum on 2 sides in 30 skulls. In this study, we classified the position of the foramen spinosum relation to sphenoid spine in more detail, as merely classifying it as lateral and medial did not provide an assessment in the anteroposterior direction, as in its normal anatomical position. The classification by Sink et al. (2023) of foramen spinosum localization is similar to our study, but they did not evaluate the relation of the sphenoid spine morphological types with foramen spinosum localization. They found posterolateral (%3.5), posteromedial (%0.39), and posteriorly (%0.78) located foramen spinosum, although we did not identify any in our skulls. While their percentages of anteromedial (%48.64), anterolateral (%20.3) and anteriorly (%14.79) located foramen spinosum are higher than in our study, the lateral placement value is close to the findings of our study (%5.84).

CONCLUSION

The relationship between foramen spinosum localization and sphenoid spine shape, as we have determined in our study, the increased lateralization of foramen spinosum in plate shaped sphenoid spine may affect the course of the middle meningeal artery, nervus spinosus, chorda tympani and auriculotemporal nerves. Therefore, variations in anatomical structures and their relationships with each other should be considered in the evaluation of pathologies in the middle cranial fossa and in the planning of surgical interventions for this region.

AUTHOR CONTRIBUTIONS

Conceptualization: Eda Duygu Ipek; Data collection and analysis: Eda Duygu Ipek, Berrin Ozustun; Manuscript writing: Eda Duygu Ipek; Manuscript review and editing: Eda Duygu Ipek, Ilgaz Akdogan; Supervision: Eda Duygu Ipek, Ilgaz Akdogan.

REFERENCES

ALMASAN O, LEUCUTA DC., DINU C, BUDURU S, BACIUT M, HEDESIU M (2022) Petrotympanic fissure architecture and malleus location in temporomandibular joint disorders. *Tomography*, 8(5): 2460-2470.

FALCON RT, RIVERA SERRANO CM, MIRANDA JF, PREVEDELLO DM, SNYDERMAN CH, KASSAM AB, CARRAU RL (2011) Endoscopic endonasal dissection of the infratemporal fossa: anatomic relationships and importance of eustachian tube in the endoscopic skull base surgery. *The Laryngoscope*, 121(1): 31-41.

FANG X, DI G, ZHOU W, JIANG X (2020) The anatomy of the parapharyngeal segment of the internal carotid artery for endoscopic endonasal approach. *Neurosurg Rev*, 43: 1391-1401.

INFANT RESHAWN I, YUVARAJ BABU K (2020) Morphometric analysis of locations, shape and variations of spine of sphenoid and its clinical importance. *Biosci Biotechnol Res Commun Special Isuue*, 13(8): 551-554.

IWANAGA J, CLIFTON W, DALLAPIAZZA RF, MIYAMOTO Y, KOMUNE N, GREMILLION HA, DUMONT AS, TUBBS RS (2020) The pterygospinous and pterygoalar ligaments and their relationship to the mandibular nerve: Application to a better understanding of various forms of trigeminal neuralgia. *Ann Anat*, 229: 151466.

LI L, XU H, JIN Y, CHEN X, CARRAU RL, LONDON JR NR (2022) Exploration of anatomical landmarks for performing an endoscopic transoral nasopharyngectomy. *Head Neck*, 44(11): 2378-2385.

LIU J, PINHEIRO-NETO CD, FERNANDEZ-MIRANDA JC, SNYDERMAN CH, GARDNER PA, HIRSCH BE, WANG E (2014) Eustachian tube and internal carotid artery in skull base surgery: an anatomical study. *The Laryngoscope*, 124(12): 2655-2664.

LIU W, CHAE R, RUBIO RR, BENET A, MEYBODI AT, FENG X, HUANG G, EL-SAYED IH (2019) Characterization of anatomical landmarks for exposing the internal carotid artery in the infratemporal fossa through an endoscopic transmasticator approach: a morphometric cadaveric study. *World Neurosurg*, 131: e415-e424.

LIU Z, YI Z (2020) A new bony anatomical landmark for lateral skull base surgery. *J Craniofacial Surg*, 31(4): 1157-1160.

RUSU MC, CIULUVICĂ, RC VRAPCIU AD, CHIRIȚĂ AL, PREDOIU M, MĂRU N (2019) Bilateral giant and unilateral duplicated sphenoidal tubercle. *Folia Morphologica*, 78(4): 893-897.

SIMONDS E, IWANAGA J, OSKOUIAN RJ, TUBBS RS, SIMONDS EA (2017) Duplication of the sphenomandibular ligament. *Cureus*, 9(10): 1-4.

ŠINK Ž, UMEK N, CVETKO E (2023) Morphometric and morphologic analysis of the foramen spinosum in the Slovenian population with clinical correlations. *Peer J*, 11: e16559.

SOPHIA MM, KALPANA R (2015) A study on foramen spinosum. *IJHSR*, 5(2): 187-193.

STAJČIĆ LS, GAČIĆ B, POPOVIĆ N, STAJČIĆ Z (2010) Anatomical study of the pterygopalatine fossa pertinent to the maxillary nerve block at the foramen rotundum. *Int J Oral Maxillofacial Surg*, 39(5): 493-496.

SUGANO GT, PAURIS CC, SILVA YBE, PANDINI FE, PALERMO RBS, BUCHAIM DV, BUCHAIM RL, CHACON EL, CASTRO CA, PAGANI BT, CUNHA MR (2022) Topographic and morphometric study of the foramen spinosum of the skull and its clinical correlation. *Medicina*, 58(12): 1740.

WORKU MG, CLARKE E (2021) Morphometric analysis of the foramen spinosum and variations of its shape, number, and relation to the spine of the sphenoid bone. *Transl Res Anat*, 24: 100124.